

Simulation Based EMI Prediction for High Speed Differential Signals

Qiaolei Huang, Jaswanth Vutukury, Deepak Pai, Gary Rara, Akshay Mohan and Jagan Rajagopalan
Amazon Lab126, 1100 Enterprise Way, Sunnyvale, CA, USA

Abstract— Electromagnetic Interference (EMI) failure is a common occurrence in electronic devices. Failing to comply with FCC/CE requirements set by government agencies delays the product time to market. Besides following proper design guidelines of layout, grounding, shielding, filtering, etc., using simulation to predict EMI failures during early design stage will greatly save time and cost. In this paper, EMI from a practical product with multiple pairs of high speed differential signals are studied. The power spectrum density of both common mode and differential mode on those differential pairs are measured. By combining with noise source information and simulated far field transfer functions, the simulated EMI can be obtained. The simulation results are later compared with measured results to show the accuracy of simulations.

Keywords—EMI, EMC, 3D simulation, differential signals, far-field probes, common mode, differential mode, consumer electronics

I. INTRODUCTION

Electromagnetic compatibility (EMC) is a major requirement for consumer electronic products set by regulatory bodies [1]-[2]. Products have to comply with these requirements to be sold in the market to avoid electromagnetic interference (EMI) with surrounding devices. In consumer electronics, time to market is crucial to get an edge over competitors. Devices have complex product design (PD), include several multi-layer PCBs, heatsinks, shield cans, flex-cables and power-supply cables [3]-[6]. Mitigating EMI failures on such devices often consumes lots of time, adds cost, and causes product delays. Thus, design for EMI plays a major role in mitigating EMI failures and launching the product in time. EMI best practices include implementing best layout design guidelines, circuit level filtering, grounding and shielding mechanisms, etc. Often, these best practices don't work as intended and require further modification. Reworking a complex device for previously mentioned changes may compromise PD integrity of the device thus changing the grounding scheme of the device which may result in inconsistent or misleading data. Some of the solutions may require spinning a new layout and building a new hardware, which is a time consuming process.

Besides following proper design guidelines of EMI, using simulation to predict EMI failures during early design stage will greatly save time and cost. An EMI simulation methodology can also help in the debugging process. EMI simulation of a single ended noise source has been studied in [1]. This paper extends the EMI simulation methodology in [1] to a more complex consumer product with multiple pairs of high speed

differential signals. The product has four pairs of high-speed differential noise sources that transmit from a complex source system to the sink system through a high speed connector. This paper also talks on how to use the correlation factor to handle EMI simulation from multiple differential lines. This paper is organized as follows. Section II describes the simulation setup for predicting EMI from differential noise source. Section III describes the simulation in the practical product with multiple pairs. Simulated EMI is obtained by combining all noise sources and its corresponding transfer functions. Simulated EMI is also compared to measured data. Section IV discusses the conclusions.

II. EMI SIMULATION SETUP

In EMI compliance measurement set-up, an antenna is placed 3 meters away from a device under test (DUT) and antenna height is varied from 1 meter to 4 meters. The DUT is placed on a turn-table which rotates 360 degrees during the measurement. In simulation, far field probes at 3 meters away are put to monitor the maximum E field from the device. As shown in Figure 1, in order to predict the EMI through simulation, knowledge of both noise source and transfer function is required. Noise source is the spectrum content of the EMI failure mode in dBm, which is usually estimated through measurement or simulation. During product development, spectrum analyzer or oscilloscope measurement can be used to obtain source information if hardware is available. If no hardware is built yet, and IBIS model or other simulation models are available, source information can be obtained from simulation. Or, if both hardware and simulation are not available, sometimes we can use simple mathematical calculation to roughly estimate source based on FFT calculation of a certain data rate.

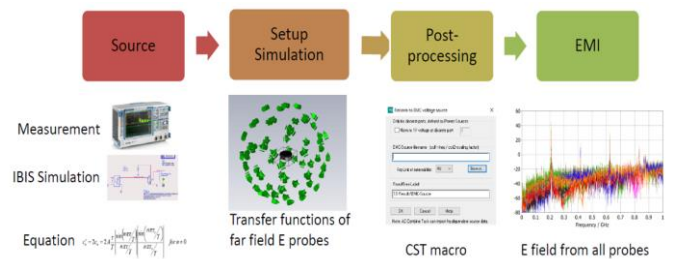


Figure 1. EMI simulation flow. EMI (dBuV/m) is obtained from noise source power (dBm) and transfer function (dBuV/m per dBm).

Transfer function is the coupling coefficient from noise source location to the far-field antenna. The unit for far field transfer function is dBuV/m per dBm. Transfer functions can be extracted in simulation using full wave solvers like CST as shown by researchers in [1]. By combining all noise sources and its transfer functions, simulated EMI can be obtained.

The simulation workflow for EMI simulation of a differential pair is described in Figure 2. The source signal is measured/simulated and imported into CST where entire 3D CAD model of the product is used for the simulation with far-field probes. In 3D simulation, the differential pair D+ and D- lanes are excited with lumped ports individually. By post process the signals with differential mode excitation (DM) and common mode excitation (CM), the corresponding transfer function can be obtained. Figure 3 shows far field probes are placed around the DUT 3 meters away. To obtain differential mode signals, Differential mode impedance is set to 100 Ω . Common mode impedance is set to be 25 Ω .

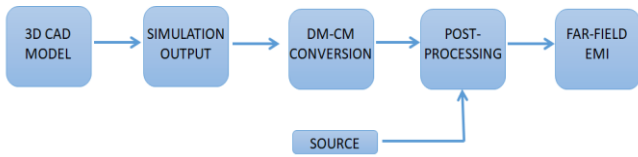


Figure 2. EMI simulation workflow for differential pair signals.

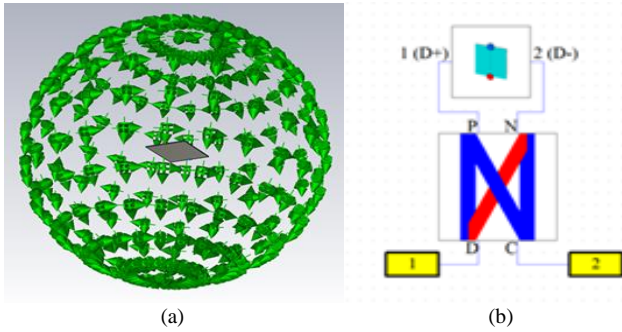


Figure 3. EMI simulation setup in CST. (a) EMI probes around the DUT; (b) schematic window in CST with single ended to DM-CM conversions. The output of the mode conversions from DM and CM signals.

III. EMI SIMULATION ON A PRACTICAL DEVICE

The simulation methodology described in Section II is applied to a practical consumer electronic product. The device has four pairs of high-speed differential signals that transition from source to sink through a connector. The connector model is shown in Figure 4. The dominant EMI noise sources in this device are found to be the high-speed signal pairs, which include three differential data pairs (D0, D1 and D2) and one differential clock pair. In this device, the maximum data rate on a differential pair is set as 5.94 Gbps. The EMI can be decomposed into differential and common mode emissions from the four pairs of signals.

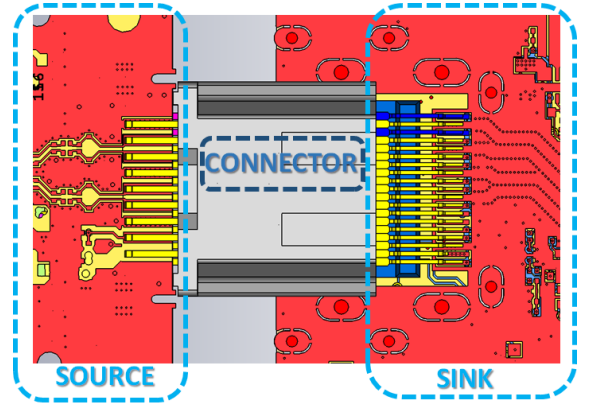


Figure 4. High speed differential pair source and sink along with connector.

The EMI radiation is obtained using the noise source power spectral density (PSD) and transfer functions. The dominant EMI noise sources in this product contain 3 differential data pairs and 1 differential clock pair. Each differential pair can be decomposed into differential mode current and common mode. In total, there are 8 possible noise sources. The EMI calculation in equation (1) contains 8 parts. In order to obtain EMI, we need to obtain 8 PSD (unit is dBm) and corresponding 8 EMI transfer functions (unit is dBuV/m per dBm). In (1), those 8 PSD include 4 common mode PSD from clock, Data 0, Data 1, Data 2; 4 differential mode PSD from clock, Data 0, Data 1, Data 2. In equation (1), 8 transfer functions (TF) include 4 common mode transfer functions from clock, Data 0, Data 1, Data 2; 4 differential mode transfer functions from clock, Data 0, Data 1, Data 2.

$$\begin{aligned}
 EMI &= \sum_{i=1}^N PSD_i \cdot TF_i = \sum_{i=1}^8 PSD_i \cdot TF_i \\
 &= PSD_{Clock_DM} \cdot TF_{Clock_DM} + PSD_{Clock_CM} \cdot TF_{Clock_CM} \\
 &+ PSD_{Data0_DM} \cdot TF_{Data0_DM} + PSD_{Data0_CM} \cdot TF_{Data0_CM} \quad (1) \\
 &+ PSD_{Data1_DM} \cdot TF_{Data1_DM} + PSD_{Data1_CM} \cdot TF_{Data1_CM} \\
 &+ PSD_{Data2_DM} \cdot TF_{Data2_DM} + PSD_{Data2_CM} \cdot TF_{Data2_CM}
 \end{aligned}$$

The source signals are measured using an oscilloscope MSOV334A which has a bandwidth of 33GHz. The data rate on each differential pair is set as 5.94 Gbps. Measured PSD for the D0 data pair is shown in Figure 5. Both differential mode and common mode are shown.

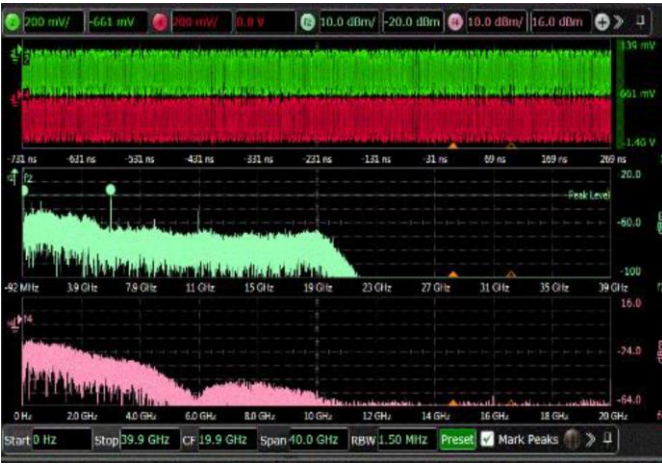


Figure 5. Measured time domain waveforms (top) and frequency domain PSD of CM (cyan color, middle) and DM (pink color, bottom) on data pair D0. Data rate on each differential pair is set as 5.94 Gbps

Although Figure 5 shows the PSD across a wide frequency range up to 15 GHz. A special focus is on 5.94 GHz. It can be observed that there is a spur at 5.94 GHz for the PSD of common mode, as shown in the middle plot of Figure 5. In the bottom of Figure 5 where differential mode is shown, no significant spur is observed. A similar trend occurs for the other data pairs. The measured DM PSD and CM PSD for all 4 differential pairs at 5.94 GHz is shown in Table 1. The CM on the clock pair is significantly smaller than CM on signal lines (~20dB lower). We believe it's due to SOC has inside low pass filter for the clock line. HDMI clock frequency is 340MHz. To minimize radiation from the high frequency, it's highly possible that SOC put a low pass filter on the clock line, thus we see minimal frequency components at 5.4GHz. SOC can't place the low pass filter on data lines. Each data line carries 5.4Gbps signal, putting low pass filter is not possible. All of the frequency components need to be kept to enable good data transmission.

In addition to measurements, we can also use the IBIS simulation to obtain PSD. The PSD from IBIS can act as cross-validations to measurement data. IBIS can be done at a very early stage of a program to obtain PSD, even before having a proto device. The IBIS simulation setup is shown in Figure 6. At 5.94 GHz, PSD from IBIS simulation is shown in Table 2. Figure 7 shows the IBIS simulated PSD of common mode and differential mode for a data pair across a wide frequency. For the PSD of both common mode and differential mode at 5.94 GHz, Table 1 and Table 2 show that the discrepancy between IBIS simulation and measurement is roughly 3dB. The accuracy in PSD is acceptable here because the real implementation in measurement domain might be slightly different than IBIS circuit simulation.

For the source PSD at 5.94 GHz, both measurement and IBIS simulation data indicate that CM PSD on 3 differential pair are the strongest among all 8 possible PSD parts. To extract all 8 transfer functions for differential and common mode, simulations were performed with the DUT model at 5.94 GHz with corresponding differential and common mode excitations.

The transfer functions for all 8 cases are shown in Table 3. Since the 4 pairs of differential signals transition from one source PCB to sink PCB through a connector, the full 3D simulations were carefully performed with dense mesh and accurate models to extract accurate transfer functions.

Table 1. Measured PSD for CM and DM of 4 differential pairs, at 5.94 GHz

Signal Pair	PSD (dBm) @ 5.94 GHz	
	Common Mode	Differential Mode
Clock	-51.4	-52.6
Data 0	-29.4	-58.3
Data 1	-29.1	-59.2
Data 2	-30.3	-62.0

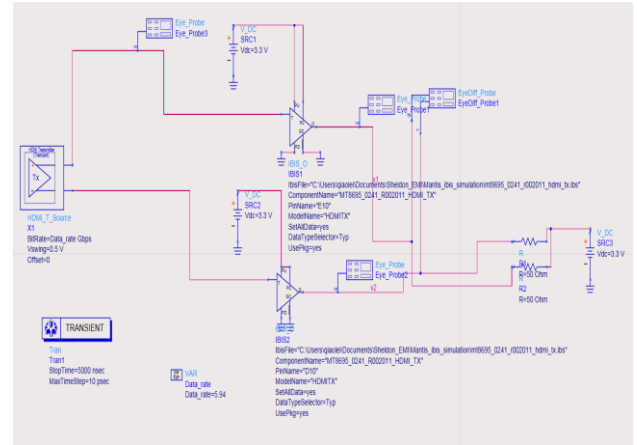


Figure 6. IBIS simulation to obtain PSD for the differential pair. The data rate for the differential pair is 5.94Gbps.

Table 2. Simulated PSD for CM and DM of 4 differential pairs from IBIS simulation, at 5.94 GHz. The clock PSD is not available in this IBIS model.

Signal Pair	PSD (dBm) @ 5.94 GHz	
	Common Mode	Differential Mode
Clock	N/A	N/A
Data 0	-27	-62
Data 1	-27	-62
Data 2	-27	-62

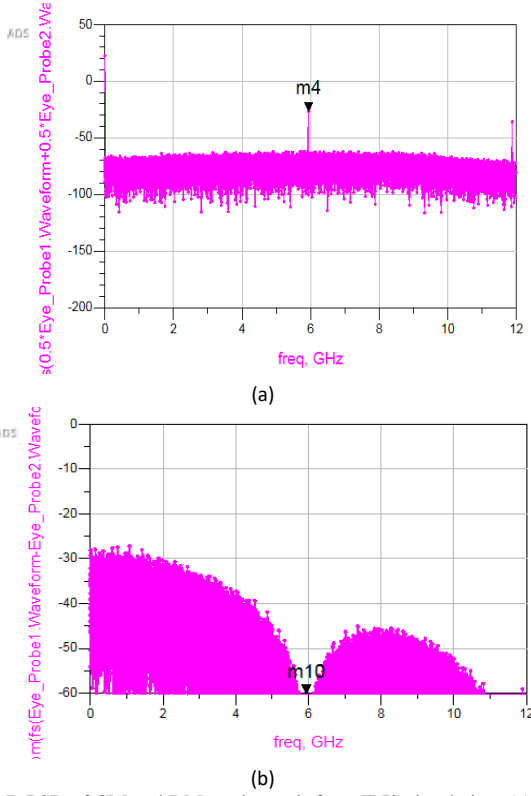


Figure 7. PSD of CM and DM on data pair from IBIS simulation, (a) is for CM PSD, (b) is for DM PSD. Data rate is 5.94Gbps. At 5.94GHz, CM PSD is simulated as -27dBm. DM PSD at 5.94GHz is -62dBm.

Table 3. Simulated transfer functions for CM and DM of 4 differential pairs, at 5.94 GHz

Signal Pair	Transfer function (dBuV/m per dBm) @ 5.94 GHz	
	Common Mode	Differential Mode
Clock	84.7	70.9
Data 0	85.5	69.7
Data 1	85.2	72.3
Data 2	85.8	73.5

At 5.94 GHz, by combining all 8 PSD from Table 1 and all 8 transfer functions from Table 3, estimated EMI can be obtained. It's also observed that 3 CM terms of the 3 data pairs are dominant out of all 8 terms in equation (1). The reason is that both PSD and transfer functions of 3 CM terms of the 3 data pairs are stronger. Namely, 8 terms in equation (1) can be simplified to only 3 terms by neglecting the much smaller 5 terms. It's also worthwhile to note that all terms in (1) are complex. Measurement or simulation of source PSD will only provide magnitude of the given source. For a single source, EMI can be calculated with only magnitude information. But for multiple sources, EMI calculation must consider the phase difference between each of the noise sources. The EMI calculation in equation (1) can be simplified to equation (2)

with 3 terms, where θ_0 , θ_1 and θ_2 are relative phases for each source term.

$$EMI = |PSD_{Data0_CM} \bullet |TF_{Data0_CM}| e^{i\theta_0} + |PSD_{Data1_CM} \bullet |TF_{Data1_CM}| e^{i\theta_1} + |PSD_{Data2_CM} \bullet |TF_{Data2_CM}| e^{i\theta_2}| \quad (2)$$

Because the data transmission is in random, θ_0 , θ_1 and θ_2 should have a random distribution from 0 to 2π . In (2), three PSD data are from Table 1, while three transfer functions are from Table 3. All possibilities of θ_0 , θ_1 and θ_2 are swept to get an EMI value of 59 dBuV/m by getting an average of all phase possibilities using equation (2). The estimated EMI across a wide frequency range is shown in Figure 8. The largest EMI happens at 5.94GHz. It's above FCC class B limit.

In [7], a similar approach to estimate EMI from multiple line cards was used to address varying phase. Since the transfer function and PSD are similar for all three data pairs, it is convenient to calculate EMI from a single pair and then adding a three-pair factor, therefore simplifying (2) to (3):

$$EMI = |PSD_{Data_CM} \bullet |TF_{Data_CM}| + 3_pair_factor \quad (3)$$

The three pair factor is calculated to be 4 dB. Note that the worst case for 3-pair case is 3 times in linear scale (9 dB in log scale) assuming 3 data pairs are transmitting the exact bit pattern and are always in phase. The actual three-pair factor from sweeping all possibilities is calculated as 4 dB, roughly half of the worst case 9 dB. In (3), the PSD data can be obtained from the average of 3 PSD data in Table 1, average transfer function can be obtained in table 2. Using (3), the EMI is estimated as 59.9 dBuV/m. These estimated EMI values bear a good correlation to the measured value of 56.77dBuV/m as shown in Table 4.

Table 4. Measured EMI for this device. Data rate at all 3 data pairs are 5.94Gbps.

Over	Limit	ReadAntenna	Cable Preamp	A/Pos	T/Pos	Remark					
Freq	Level	Limit	Line	Level	Factor	Loss	Factor	cm	deg		
MHz	dBuV/m	dB	dBuV/m	dBuV	dB/m	dB	dB	cm	deg		
1	5940.00	60.17	-13.83	74.00	73.20	32.44	11.59	57.06	100	301	Peak
2 *	5940.00	56.77	2.77	54.00	69.80	32.44	11.59	57.06	100	301	Average

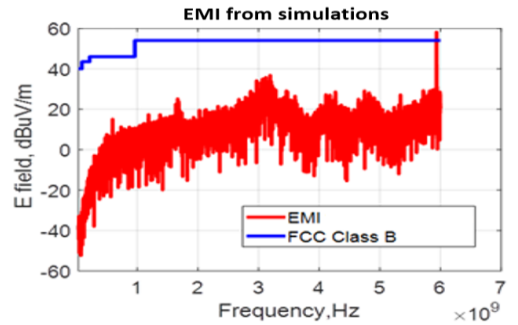


Figure 8. Estimated EMI from equation (2), compared to FCC class B limit.

As the EMI are dominated by common mode radiations on 3 data pairs, common mode chokes are added at 3 data pairs to reduce EMI. The same procedures of EMI estimation are repeated for with common mode choke case. With common mode choke which works at 5.4 GHz, the measured EMI and simulated EMI are 40 dBuV/m and 37.2 dBuV/m. We also measured and simulated EMI for another data rate. All 3 data pairs are set to the data rate of 2.2Gbps, measured EMI and simulated EMI are 45 dBuV/m and 40.4 dBuV/m. Overall, around 5dB of estimation accuracy is achieved for different test cases.

IV. CONCLUSION

This paper presents a simulation methodology for predicting EMI failures in a complex practical consumer electronic product. This product has multiple pairs of differential high-speed signals. The simulated EMI correlates within around 5 dB compared to measurement. With accurate EMI prediction methods, product design engineers can come up with targeted mitigation methods, and thereby saving design cost and time to market.

REFERENCES

- [1] Q. Huang et al., "Accurate Prediction and Mitigation of EMI from High-Speed Noise Sources using Full Wave Solver," in Proc. of IEEE Symp. Electromagn.Compat., 2019, pp. 595-599
- [2] G. Shen, S. Yang, J. Sun, S. Xu, D. J. Pommerenke and V. V. Khilkevich, "Maximum Radiated Emissions Evaluation for the Heatsink/IC Structure Using the Measured Near Electrical Field," IEEE Trans. Electromagn. Compat., vol. 59, no. 5, pp. 1408-1414, Oct. 2017
- [3] C. Hwang and Q. Huang, "IC placement optimization for RF interference based on dipole moment sources and reciprocity," 2017 Asia-Pacific International Symposium on Electromagnetic Compatibility (APEMC), Seoul, 2017, pp. 331-333.
- [4] Q. Huang et al., "Radiated Spurious Emission Prediction Based on Dipole Moment and Full Wave Simulation," in Proc. of IEEE Int. Symp. Electromagn.Compat., 2020, pp. 646-649.
- [5] A. Huang et al., "Investigation and Mitigation of Radio Frequency Interference Caused by Weak Grounding of USB Type-C Receptacle Connector," in Proc. of IEEE Symp. Electromagn.Compat., 2020, pp. 139-144.
- [6] Q. Huang, T. Enomoto, S. Seto, K. Araki, J. Fan and C. Hwang, "Physics-Based Dipole Moment Source Reconstruction for RFI on a Practical Cellphone," IEEE Trans. Electromagn. Compat., vol. 59, no. 6, pp. 1693-1700, Dec. 2017.
- [7] J.Meiguni et al., " System Level EMC for Multiple EMI Sources," in Proc. of IEEE Int. Symp. Electromagn.Compat., 2019, pp. 493-498.